



Volume 76 Issue 6 June 2007 ISSN 0969-806X

# Radiation Physics and Chemistry

The journal for Radiation Physics, Radiation Chemistry and Radiation Processing  
A multidisciplinary journal linking science and industry



## Editors

M. J. COOPER  
D. CREACH  
J. FARKAS  
J. FERNÁNDEZ-VARELA  
J. I. GARNETT  
L. GERWARD  
N. GETOFF  
D. I. L. JONES  
I. KARTSU  
J. KRÓI  
B. J. LYONS  
S. T. MANNON  
L. MUSILEK  
P. NETA  
D. RAZEM  
S. C. ROY  
P. SUARPE  
A. SINGH  
Y. TABAJA  
A. TALLENTIRE  
A. D. TRIFUNAC

## Editors-in-Chief

Radiation Physics: P. M. Bergstrom, Jr  
Radiation Chemistry: L. Wojnárovits  
Radiation Processing: A. Miller

## Consulting Editor

J. H. Hubbell



Radiation Physics and Chemistry is a journal recognised  
by the International Radiation Physics Society

<http://www.elsevier.com/locate/radphyschem>

This article was originally published in a journal published by Elsevier, and the attached copy is provided by Elsevier for the author's benefit and for the benefit of the author's institution, for non-commercial research and educational use including without limitation use in instruction at your institution, sending it to specific colleagues that you know, and providing a copy to your institution's administrator.

All other uses, reproduction and distribution, including without limitation commercial reprints, selling or licensing copies or access, or posting on open internet sites, your personal or institution's website or repository, are prohibited. For exceptions, permission may be sought for such use through Elsevier's permissions site at:

<http://www.elsevier.com/locate/permissionusematerial>



# The effect of encounters involving ions, excited molecules, and neutral radicals in a track on the delayed fluorescence of irradiated alkane solutions

V.I. Borovkov<sup>a,b,\*</sup>, K.A. Velizhanin<sup>b</sup>

<sup>a</sup>*Institute of Chemical Kinetics and Combustion, SB RAS, Novosibirsk 630090, Russian Federation*

<sup>b</sup>*Novosibirsk State University, Novosibirsk 630090, Russian Federation*

Received 3 April 2006; accepted 27 September 2006

## Abstract

A computer model has been developed to simulate the processes of the excited states formation in irradiated alkane solutions. The model includes the charge and energy transfer reactions as well as intratrack encounters involving excess electrons, radical ions, the excited states of molecules, and neutral radicals including spin effects. The model is applied to visualize the contact interactions and to establish their effect on the delayed fluorescence decay in nanosecond time domain after pulsed irradiation. The model predicts no significant influence of neutral alkyl radicals on the delayed fluorescence.

© 2006 Elsevier Ltd. All rights reserved.

**Keywords:** Radiation track; Computer simulation; Radical ions; Excited states; Delayed fluorescence

## 1. Introduction

The ionizing radiation of organic solutions is a widely applied method to generate short-lived reactive species, such as radical ions, neutral radicals, and excited states of molecules (Shkrob et al., 2001; Mozumder, 1999; Brocklehurst, 1992a,b; Yoshida et al., 1991; Sauer et al., 1991; Singh, 1972). At present, a qualitative pattern of the process initiated by an ionizing particle in solution is well known. Various techniques have been used to establish the stages of radiolysis, intermediates involved, as well as the characteristic times of radiation-induced chemical reactions.

At the same time, as discussed by Shkrob et al. (2001), some of the fundamental problems of alkane radiolysis are still not clear. Among them there are two closely related problems of the determination of the detailed structure of the ionizing particle track and the role of intratrack interactions between short-lived intermediates. More atten-

tion has been paid to the first problem. The experimental approaches used were the analysis of the value of the yield of free ions (Holroyd and Sham, 1985; Freeman, 1987; Gee et al., 1988; Hummel and Bartczak, 1988; Bartczak and Hummel, 1997; Siebbeles et al., 1997) or the excited states of various multiplicity as well as the estimations of geminate recombination probability (Lozovoy et al., 1990; Sauer et al., 1991; Brocklehurst, 1992b; Bartczak and Hummel, 1993; Sauer and Jonah, 1994; Holroyd et al., 1997).

Our study is focused on the role of the contact interactions between intermediates in a track in order to establish their effect on the delayed fluorescence decay in nanosecond time domain after an irradiation pulse. Such an investigation is believed to be instructive for the experimental techniques like optically detected ESR, the method of time-resolved magnetic field effects (TR-MFE), etc., which analyze the delayed fluorescence of irradiated solutions (Anisimov, 1991; Brocklehurst, 1997; Borovkov et al., 2003; Bagryansky et al., 2004).

Using the computer simulation of intratrack reactions, we discuss the cases of both a pure solvent, which is similar in its parameters to *n*-dodecane and the solutions of an electron donor whose molecules are luminophor also.

\*Corresponding author. Institute of Chemical Kinetics and Combustion, SB RAS, Novosibirsk 630090, Russian Federation. Fax: +7 3833 307 350.

E-mail address: [borovkov@kinetics.nsc.ru](mailto:borovkov@kinetics.nsc.ru) (V.I. Borovkov).

Tetramethyl-*para*-phenylenediamine (TMPD) was taken as electron donor prototype. Additionally, we discuss the influence of the external magnetic and electric fields on the delayed fluorescence decays of the luminophore solution.

To simulate the delayed fluorescence decays, three channels of the formation of singlet excited luminophore molecules were considered:

- (1) recombination of (solute radical cation/excess electron) pairs;
- (2) radiationless energy transfer from singlet excited solvent molecules;
- (3) annihilation of triplet-excited molecules of luminophore (TTA).

As reactive intermediates excess electrons, excited solute and solvent molecules, radical ions, neutral radicals were considered. Encounters of the intermediates were assumed to affect the delayed fluorescence mainly via quenching of the excited states and spin correlation decay.

The up-to-date development of computation techniques allowed radiation track modeling *ab initio*, starting with an ionizing particle and calculating the whole track structure using the data on the cross-sections of the interaction between electrons of various energies and solvent molecules (Pimblott and Green, 1996; Siebbeles et al., 1997). However, the modeling of all subsequent radiation-induced reactions and, especially, the analysis of the calculated results are likely to be grave tasks even when using the modern computers. In any case, it is to be instructive to have information on the relative contributions of different parts of a radiation track to an observed response. Besides, it should be noted that only closely located particles are sure to interact within nanoseconds. Being guided by this prudential, in the present work we have examined the radiation-induced processes as proceeding in isolated spherically shaped spurs of different sizes constituted from different numbers of primary ion pairs. This approximation was frequently used in the earlier simulations (Schmidt, 1983; Lozovoy et al., 1990; Sauer et al., 1991; Anishchik et al., 1996; Bartczak and Hummel, 1997; LaVerne et al., 1997).

## 2. Description of the model

As it was mentioned in Section 1, the computer simulation of the diffusion-drift motion of ions and other active species started from spherically shaped spur. The reactive species whose spatial position was processed in the program were excess electrons ( $e^-$ ), radical cations ( $S^{+\bullet}$ ,  $D^{+\bullet}$ ), the singlet and triplet excited states of solvent and solute ( $^1S^*$ ,  $^1D^*$ ), respectively. As parameters for modeling we took the spur radius  $R_S$ , the number  $N_0$  of initial (cation/electron) pairs in the spur, the diffusion coefficients of neutral particles and the charge carriers involved, the hard-core radii of the species, solute concentration, and the lifetimes of the singlet excited states.

Lifetime of  $^3D^*$  was assumed to be infinitely large while any  $^3S^*$  was considered to decay immediately with the formation of the pair of neutral radicals  $^3(R^{\bullet}\cdot R^{\bullet})$  (Schwarz et al., 1981; Mehnert, 1991; Brocklehurst, 1992a; LaVerne et al., 1997). The values of the diffusion coefficients of molecular particles were taken to be close to those typical of liquids with a viscosity of about 1 cP. We also assumed that excited and neutral molecules move twice as quickly as corresponding ions (Terazima et al., 1995; Ukai et al., 2000). The individual parameters of reactive species are listed in Table 1. The value of the mobility of excess electrons used in these calculations is two times as low as that published in Gee et al. (1988). On the other hand, it is close to the value estimated using the method of time-resolved electric field effect (Borovkov et al., 1997).

While modeling, typically  $10^5$ – $10^6$  cycles of calculations of the displacements of particles and their encounter reactions were repeated starting from the initial configuration until the time domain of interest came to its end or all reactive species disappeared. The initial configuration for a cycle was generated as the random distribution of solvent radical cations inside a sphere of a given radius  $R_S$  (2–50 nm) and the isotropic distribution for excess electrons with the radial distribution function  $f(r > a) = 1/b \exp(-(r - a)/b)$  around corresponding parent cation. Here  $b = 6$  nm, and the parameter  $a = 1$  nm was the closest distance between ions. The subsequent reactions of reactive species, e.g. their recombination, electron or electronic energy excitation transfers, singlet–triplet conversion or spin exchange are listed in Table 2. Reaction (1) was the immediate result of ionizing irradiation with a singlet spin correlation between the geminate solvent hole and excess electron.

The algorithm used in our work to describe the reactions between the intermediates, was similar to that described previously (Lozovoy et al., 1990; Anishchik et al., 1996). The displacement of charge carriers during a program step by time  $\Delta t$  was calculated as the vector sum of the randomly oriented diffusion shift with the mean square value  $(6D\Delta t)^{1/2}$  and the drift motion  $\mu(\mathbf{E} + \mathbf{E}_0)\Delta t$ . Here,  $\mathbf{E}$  is the Coulomb field of other charges in the spur and  $\mathbf{E}_0$  is external electric field, which was believed not to affect the

Table 1  
The diffusion coefficients ( $D$ ), mobilities ( $\mu$ ), and radii ( $R$ ) of the particles involved in spur reactions (1)–(25) presented in Table 2<sup>a</sup>

Particle	$D$ (cm <sup>2</sup> /s)	$\mu$ (cm <sup>2</sup> /Vs)	$R$ (nm)
$S^{+\bullet}$	$5 \times 10^{-6}$	$2 \times 10^{-4}$	0.5
$e^-$	$2.5 \times 10^{-4}$	$10^{-2}$	0.5
$D^{+\bullet}$	$5 \times 10^{-6}$	$2 \times 10^{-4}$	0.5
$^1S^*$	$1 \times 10^{-5}$	—	0.5
$^1,3D^*$ , D	$1 \times 10^{-5}$	—	0.5
$R^{\bullet}$	$5 \times 10^{-6}$	—	0.5

<sup>a</sup>S is the solvent molecule,  $e^-$  is the excess electron, D (Roman type) is the hole acceptor molecule,  $S^*$  and  $D^*$  are the molecules in excited states with their multiplicity indicated,  $R^{\bullet}$  is the neutral radical resulting from the decay of triplet excited solvent molecule.

Table 2  
Reaction scheme, probabilities for encounter reactions, and rate constants used in modeling<sup>a</sup>

No.	Reaction	Reaction probability or rate constant
1	$S \rightarrow S^{+\bullet} + e^{-}$	—
2	$S^{+\bullet} + e^{-} \rightarrow {}^1,3S^*$	1 <sup>b</sup>
3	$S^{+\bullet} + (D, {}^1,3D^*) \rightarrow S + D^{+\bullet}$	1/3 ( ${}^3D^*$ ), 1 ( ${}^1D^*$ ), $7.6 \times 10^9/M/s$ ( $D$ ) <sup>c</sup>
4	$D^{+\bullet} + e^{-} \rightarrow {}^1,3D^*$	1 <sup>b</sup>
5	${}^1S^* \rightarrow {}^3S^*$	$2.5 \times 10^8 s^{-1}$
6	${}^1S^* + D \rightarrow S + {}^1D^*$	$1.1 \times 10^{10}/M/s$ <sup>c</sup>
7	${}^1D^* \rightarrow {}^3D^*$	$1.8 \times 10^8 s^{-1}$
8	${}^1D^* \rightarrow D + h\nu$	$2 \times 10^7 s^{-1}$
9	${}^3D^* + {}^3D^* \rightarrow D + {}^1D^*$	1/9
10	${}^3D^* + {}^3D^* \rightarrow D + {}^3D^*$	1/3
11	${}^1D^* + {}^3D^* \rightarrow {}^3D^* + {}^3D^*$	1/3
12	${}^1D^* + {}^1D^* \rightarrow {}^3D^* + {}^3D^*$	1/9
13	${}^1S^* + {}^3D^* \rightarrow {}^3S^* + {}^3D^*$	1/3
14	${}^1S^* + {}^1S^* \rightarrow {}^3S^* + {}^3S^*$	1/9
15	$(S^{+\bullet}, D^{+\bullet}, e^{-})\uparrow + {}^1S^* \rightarrow (S^{+\bullet}, D^{+\bullet}, e^{-})\downarrow + {}^3S^*$	1/3
16	$(e^{-}, D^{+\bullet})\uparrow + {}^1D^* \rightarrow (e^{-}, D^{+\bullet})\downarrow + {}^3D^*$	1/3
17	$(e^{-}, D^{+\bullet})\uparrow + {}^3D^* \rightarrow (e^{-}, D^{+\bullet})\downarrow + {}^3D^*$	2/3
18	${}^3S^* \rightarrow R^*\uparrow + R^*\uparrow$	Instantaneous process
19	$R^* + R^* \rightarrow \text{Products}$	1/4
20	$S^{+\bullet}\uparrow + R^*\downarrow \rightarrow S + R^+\uparrow$	1/4
21	$e^{-}\uparrow + R^*\downarrow \rightarrow R^{-}$	1/4
22	$D^{+\bullet}\uparrow + R^*\downarrow \rightarrow D^{+\bullet}\downarrow + R^*\uparrow$	1/2
23	$R^*\uparrow + ({}^1D^*, {}^1S^*) \rightarrow R^*\downarrow + ({}^3D^*, {}^3S^*)$	2/3
24	$R^+ + e^{-} \rightarrow R^*$	1
25	$(S^{+\bullet}, D^{+\bullet}) + R^{-} \rightarrow (S, D) + R^*$	1

<sup>a</sup>The probabilities for encounter reactions are dimensionless.

<sup>b</sup>Probability of the recombination is given. Spin multiplicity is determined by spin correlation (see text).

<sup>c</sup>For reactions (3) and (6) involving solute molecules in their ground state the rate constants were calculated as  $k(t) = 4\pi R_0 D_0 (1 + R_0/(\pi D_0 t)^{1/2})$ , where  $R_0$  was the corresponding reaction radius and  $D_0$  was the sum of the diffusion coefficients of the reacting particles.

initial electron distribution. The value  $\mu$  of the mobility of charge carriers was calculated from the Nernst–Einstein relationship  $\mu/e = D/kT$ . The value of  $\Delta t$  was chosen short enough to ensure that the distance between any particles after a single step was changed by no more than 10% and the probability of reactions (2)–(25) did not exceed 0.1. No changes in the obtained results were observed with the use of more rigid timing constraints.

In the program, the distances between all types of active particles were controlled. It was assumed that the collision as well as possible reaction occurred when the distance between the particles was shorter than  $R_0$  being the sum of corresponding species' radii including energy transfer reactions (Mehnert et al., 1988). The encounter of particles discontinued if the distance increased by more than 0.1 nm as compared with the reaction radius  $R_0$ . Such an interpreting for the particles' contact was somewhat conventional but it allowed estimating the relative contributions of different kinds of pairs.

All bimolecular reactions, including the reactions of charge recombination (2) and (4), were assumed to occur at the contact of reagents with the conservation of the pair's spin multiplicity while going from the reagents to reaction product(s) (Molin, 1984; Okamoto et al., 2001). The reaction probabilities at the first encounter of nonspin-correlated particles are given in Table 2. In some cases, the only result of a particle encounter was the change in particle spin state as

indicated with ( $\uparrow$ ) or ( $\downarrow$ ) in Table 2. If such a spin exchange involved a radical ion (or an electron), from that moment the geminate pair containing that radical ion was considered as non-spin-correlated. For simplicity, no spin correlation between the species was taken into account for reencounters. The reaction involving acceptor molecules in their ground state was described as a quasi-monomolecular reaction with a time-dependent rate constant  $k(t) = 4\pi R_0 D_0 (1 + R_0/(\pi D_0 t)^{1/2})$ , where  $D_0$  was the sum of the reagent diffusion coefficients. A value of 5 ns was chosen as  ${}^1D^*$  lifetime and the rate of internal conversion (reaction 7) was assumed to be nine times as high as that of fluorescence emission (reaction 8) to result in solute fluorescence quantum yield of 10% as for TMPD (Potashnik et al., 1969). For  ${}^1S^*$  these parameters were 4 ns and 0.5%, respectively (Rothman et al., 1973; Barigelletti et al., 1979; Holroyd et al., 1997).

The output of the program was the collection of histograms for moments of all reactions (2)–(25). Note, that reaction (8) gave the delayed fluorescence intensity of the solvent irradiated. Recombination moments of excess electron and the radical cations were recorded in different files depending on the fact whether these charge carriers arose as geminate pair or not. We assumed that for the nongeminate (cross) pairs as well as geminate ones in which the spin correlation was lost due to the spin exchange with a third particle, the probability of the single excited molecule formation upon recombination was 0.25 in any

case. For the geminate pairs  $S^{+\bullet}/e^-$ , it was assumed that pairs always recombined in the singlet state since the majority of the pairs recombined within a subnanosecond range and singlet–triplet conversion was unlikely to occur. On the other hand, for secondary geminate pairs  $D^{+\bullet}/e^-$ , the probability of singlet excitation formation was assumed to be 0.5 and 0.25 in nonzero magnetic field and zero field, respectively. These values corresponded to the case of high rate of singlet–triplet transitions due to either strong hyperfine interactions or phase relaxation, i.e. the case of large ESR spectrum width for  $D^{+\bullet}$  (Anisimov, 1991; Bagryansky et al., 2004). The model included neither the spin lattice relaxation of radicals nor the dipole–dipole interaction of various particles with spin as well as any effects determined by spin correlation of different radical ion pairs (Brocklehurst, 1992a). The effect of the latter factor was believed insignificant in a spur when the fast phase paramagnetic relaxation was included.

### 3. Results and discussion

#### 3.1. Formation and lifetime of singlet excited solvent states in pure solvent

In this section, we will consider the processes of the formation of singlet excited solvent molecules  $^1S^*$  in a pure

solvent. The particular attention will be paid to the effect, which the local ionization density and particles' encounters have on the yield and lifetime of  $^1S^*$ .

Figs. 1(a)–(d) show (in semilogarithmic scale) the calculated time dependences of the recombination rates of the geminate and the nongeminate ion pairs at  $N_0 = 5$  (a, b) and  $N_0 = 15$  pairs (c, d), respectively, at  $R_S = 5$  nm. Figs. 1(a) and (c) also compare the recombination rate of a single pair  $S^{+\bullet}/e^-$  for the same other parameters. The numbers of the simulation cycles for all the cases presented in Fig. 1 were chosen to make the numbers of initial pairs  $S^{+\bullet}/e^-$  equal to  $1.5 \times 10^6$ .

In the time domain studied, most of the recombining pairs are  $S^{+\bullet}/e^-$ . As compared to total ion recombination rate, the contribution of all other pairs, involving the products of the primary charges scavenging by neutral radicals, reaches about 20% towards 10 ns for  $N_0 = 5$ . For a denser spur, this value amounts to about 40%. Being integrated over a very long interval, the amounts of the pairs recombined, which differ from  $S^{+\bullet}/e^-$ , are 2% for the case of  $N_0 = 5$  and 2.5% for  $N_0 = 15$ .

To demonstrate the relative contributions of  $^1S^*$  encounters with various species to the rate of the singlet–triplet conversion of  $^1S^*$ , in Figs. 2(a) and (b) the time dependences of the encounters number per 0.1 ns are shown for the spurs considered above. In the model applied, at times  $< 0.25$  ns, most often are the encounters

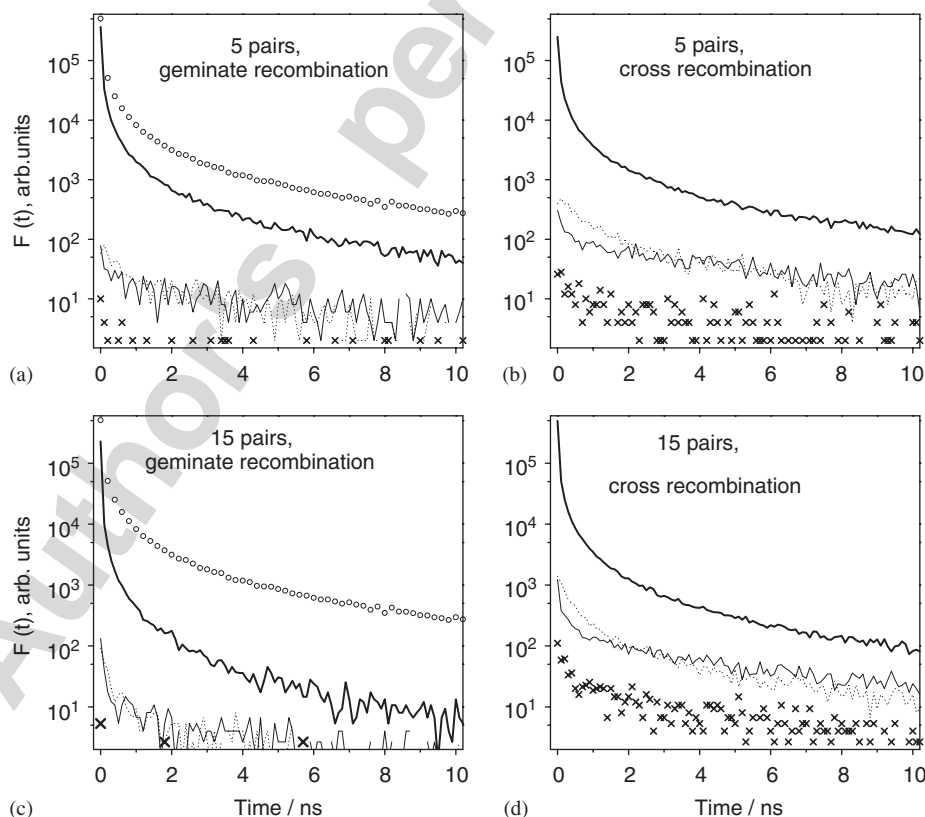


Fig. 1. The time dependence for counts of geminate (a, c) and cross (b, d) ion pairs recombination per 0.1 ns at  $N_0 = 5$  (a, b) and  $N_0 = 15$  pairs (c, d) in the spur with  $R_S = 5$  nm in pure solvent. All the figures show the recombination rates of the pairs (from top to bottom):  $S^{+\bullet}/e^-$  (thick line),  $S^{+\bullet}/R^-$  (thin line),  $R^+/e^-$  (dotted line),  $R^+/R^-$  ( $\times$ ). The cycle number of simulation were  $3 \times 10^5$  and  $10^5$  for  $N_0 = 5$  and 15, respectively. In parts (a) and (c) circles ( $-$ ) denote the recombination rate of an isolated  $S^{+\bullet}/e^-$  pair with all other parameters being the same ( $1.5 \times 10^6$  cycles).

between  $^1S^*$  and electrons (curves 1), or solvent holes (curves 2). Later, the encounters between the excited molecules and neutral radicals (curves 3) become the main channel of the conversion. The encounters involving two excited solvent molecules (curves 4) are comparatively infrequent. As follows from Fig. 2(a) and (b), the number of collisions of  $^1S^*$  with other particles increases considerably with increasing spur density but the relative contributions of the different pairs remain approximately the same.

Figs. 3(a)–(d) show the effect of spur size  $R_S$  and the number of initial ion pairs  $N_0$  on the delayed fluorescence from the other viewpoint. Parts 3a and b demonstrate the time dependences of the number of  $^1S^*$  divided by  $N_0$  for various  $R_S$  (3a) and  $N_0$  values (3b). These dependences are to coincide to within a coefficient with the delayed fluorescence decays of the solvent irradiated. Fig. 3a shows the calculated results at  $N_0 = 5$  for  $R_S$  varied from 2 to 10 nm, and Fig. 3b shows these as calculated for  $R_S = 5$  nm and  $N_0$  varied from 3 to 15.

Fig. 3b also compares the calculated result for the isolated pair with the approximation of this dependence by exponential function over the range 1–5 ns. Such approximation is likely to be typical procedure for obtaining the value of excited state lifetime. A characteristic decay times was obtained to be 5.04 ns, which is larger than  $^1S^*$  lifetime assumed in the model. The “observed” decay time exceeds 4 ns due to the fact that with the used electron mobility only 80% of  $S^{+\bullet}/e^-$  pairs recombine until 1 ns and some  $^1S^*$  are formed at  $t > 1$  ns. The proportion between the contributions of electron ion pair’s recombination and  $^1S^*$  quenching due to encounters determines the “observed” lifetime of this species.

Formally applying the same procedure of the exponential approximation over the range 1–5 ns to curves 1–5 in Fig. 3b, one obtains the values of 3.4, 3.6, 3.8, and 4.0 ns, respectively. For curves 1–5 in Fig. 3a, this approximation provides the following “observed” lifetimes: 3.9, 3.8, 4.0, 4.2, and 4.4 ns, respectively.

In Figs. 3c and d, the time dependences of the  $^1S^*$  decay rates as referred to the decay rate of isolated singlet

excitation ( $0.25 \text{ ns}^{-1}$ ) are shown. The numbering of the curves coincides with that for parts (3a) and (3b).

Obviously, the contribution of the encounters to the rate of the singlet–triplet conversion of  $^1S^*$  is high only at times  $< 1$  ns. According to the results presented in Figs. 2a and b, it implies that at the short times the most important processes of  $^1S^*$  quenching are the encounters with either electrons or solvent holes. These encounters determine the “observed” yield of the solvent excited state while those with neutral radicals in later moments result in a moderate shortening of the mean fluorescence lifetime of the excited state.

Also note that in the experiment reported in Holroyd et al. (1997), the lifetime of the singlet excited alkane molecule was determined from the delayed fluorescence decay assuming an instantaneous formation of excitations even for solvents with comparatively low electron mobility. At the same time, as follows from the presented results, the recombination of electrons can have substantial effect on the observed lifetime of the excited states.

### 3.2. Formation of the solute excited states

The processes discussed in the previous section are closely related to those occurring in the solution of electron donor, which is also both the acceptor of electronic energy excitations and the luminophor. Figs. 4a and b show the contributions of different pairs to the yield of solute singlet excited molecules  $^1D^*$  for the acceptor concentrations of 1 mM (4a) and 20 mM (4b), respectively. The calculations were performed for  $R_S = 5$  nm and  $N_0 = 5$  for  $10^6$  calculation cycles. The contributions are:

- (1) the energy transfer from  $^1S^*$  to the acceptor via the sequence of reactions (1)–(2)–(6);
- (2) the recombination of  $D^{+\bullet}/e^-$  pairs via reactions (1)–(3)–(4), the contributions of the geminate and cross pairs are presented separately;
- (3) triplet–triplet annihilation (9).

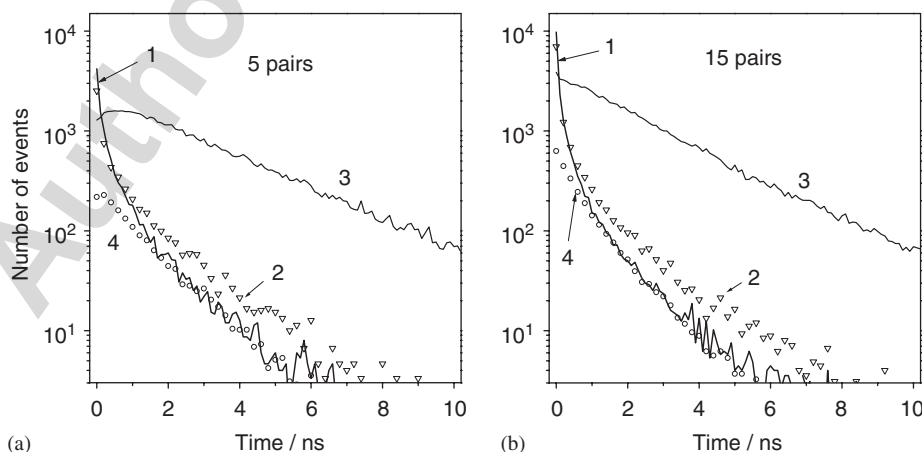


Fig. 2. The counts (per 0.1 ns) of the particles’ encounters resulting in  $^1S^*$  singlet–triplet conversion for  $N_0 = 5$  (a) and  $N_0 = 15$  pairs (b) in a spur with  $R_S = 5$  nm in pure solvent. Both of the parts show the encounters of  $^1S^*$  with  $e^-$  (curves 1),  $S^{+\bullet}$  (curves 2, triangles),  $R^\bullet$  (curves 3), as well as with other  $^1S^*$  molecules (curves 4, circles).

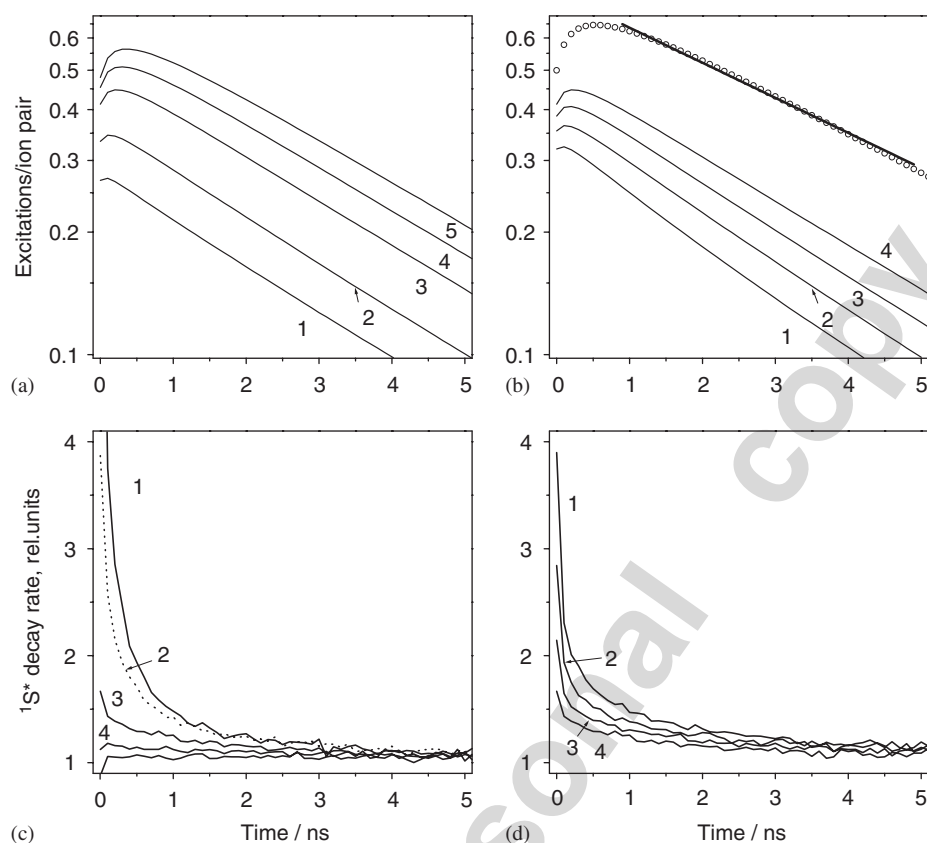


Fig. 3. (a) The time dependence of the number of  $^1S^*$  (divided by  $N_0 = 5$ ) in the spur with  $R_S = 2$  nm (curve 1),  $R_S = 3$  nm (curve 2),  $R_S = 5$  nm (curve 3),  $R_S = 7$  nm (curve 4), and  $R_S = 10$  nm (curve 5) in pure solvent; (b) the same in the spur with  $R_S = 5$  nm for  $N_0 = 15$  pairs (curve 1),  $N_0 = 10$  pairs (curve 2),  $N_0 = 7$  pairs (curve 3),  $N_0 = 5$  pairs (curve 4), and  $N_0 = 1$  pair (circles) in the absence of acceptors. For the isolated pair, the exponential approximation over the range 1–5 ns (solid line) is shown. (c, d) The time dependences of the  $^1S^*$  decay rates in the spurs, whose parameters are the same as presented in parts (a) and (b), respectively, referred to the decay rate of isolated singlet excitation ( $0.25 \text{ ns}^{-1}$ ). The numeration of the curves coincides with that for (a) and (b) (curve corresponding to number 5 is not designated).

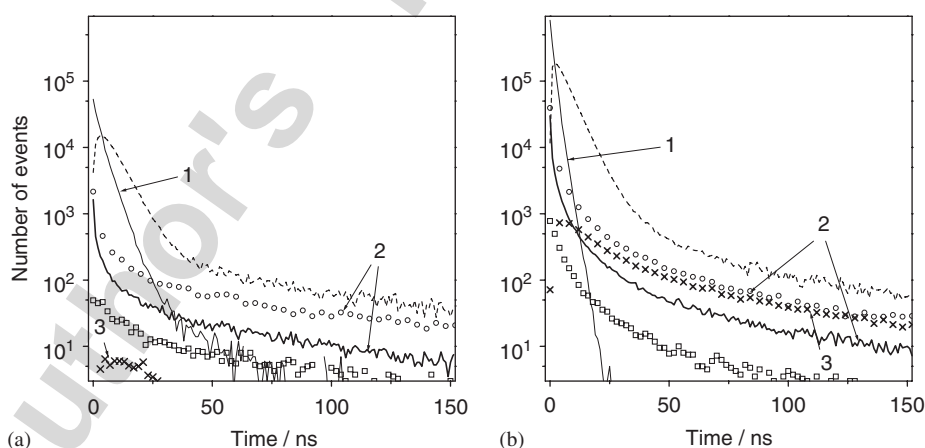


Fig. 4. The time dependences of the numbers of  $^1D^*$  formation per 1 ns calculated for  $10^6$  cycles at  $N_0 = 5$ ,  $R_S = 5$  nm, and  $[D] = 1 \text{ mM}$  (a) and  $[D] = 20 \text{ mM}$  (b). Curves 1: the contribution of energy transfer via reaction (6); curves 2: recombination of geminate (solid line) and cross (circles) pairs  $D^+ \cdot / e^-$ ; curves 3, ( $\times$ ):  $^3D^*$  annihilation in reaction (9). The figure also shows the recombination rates for all the pairs in reactions (24) and (25) (squares) as well as  $^1D^*$  fluorescence intensity (dashed line, with  $10 \times$  magnification).

For comparison, Figs. 4a and b give the recombination rate for pairs involving ion-non-radicals (reactions (24) and (25)). The total calculated fluorescence decays are shown in both parts of Fig. 4 by dashed lines with  $10 \times$  magnification.

Interestingly, at the used model parameters, the delayed fluorescence intensity at times to about 40 ns resembles a quasi-exponential process. This is the fluorescence of  $^1D^*$  species created within a few early nanoseconds mostly via energy transfer from  $^1S^*$  (reaction 6). Regardless of the fact

that the lifetimes of both  $^1S^*$  and  $^1D^*$  are comparatively short, this effect appears because the rate of the reaction (6) initially is extremely high. Though the rate decreases drastically, this dominates any other reactions for 10 ns, at least. Thus several lifetimes should pass before the decay of the promptly created  $^1D^*$  allows one to reveal the fluorescence of  $^1D^*$  being formed via reaction (4) or (9) in later moments. The prompt recombination of  $D^{+\bullet}/e^-$  pairs contributes to this quasi-exponential component in minor extent.

As follows from these results, an increase in the acceptor concentration causes a noticeable increase in the contributions of both the processes of energy transfer (curves 1) and triplet–triplet annihilation (curves 3). Importantly, the contribution of TTA process, which is a bimolecular one, depends on solute concentration in a greater extent as compared to ion pair recombination. Thus, the further increase in solute concentration should result in the increase of relative importance of the annihilation of  $^3D^*$  that have arisen in the same spur.

To this, we can add that the long-time dependences of the rate for both the recombination of the ion pairs and TTA are similar although the diffusion coefficients of the particles involved are different by two orders of magnitude. This is a known regularity of geminate diffusion-controlled processes (Hong and Noolandi, 1978; Ovchinnikov et al., 1989). If the electron mobility increases the rate of ion pair recombination at, e.g.  $t > 50$  ns, decreases with respect to  $^3D^*$  annihilation in whole of the time domain.

### 3.3. The role of intraspur encounters

To discuss further the effect of electric and magnetic fields on the delayed fluorescence decay, it is appropriate to discuss first how the intratrack encounters affect the geminate ion recombination as well as the TTA. The

former is the only reaction, whose yield is sensitive to the external magnetic field. As it will be shown below, TTA process is not sensitive significantly to both the electric field and the magnetic one. Thus, the contributions of these channels affect the magnitude of the field effects.

In Fig. 5a, the time dependences of the recombination rates of the geminate and cross pairs  $D^{+\bullet}/e^-$  (groups of the curves 1 and 2, respectively) are presented for  $R_S = 5$  nm and  $N_0 = 5$  at  $[D] = 20$  mM. Fig. 5b shows the collisions frequency of  $^3D^*$  in the same conditions. The solid lines in both parts denote the results obtained with taking into account all reactions (1)–(25). Circles denote the results obtained with account for the reactions (1)–(17) only, i.e., neglecting any appearance of neutral radicals. The dashed line shows the dependences calculated for the case when only reactions (1)–(11) are allowed. The latter case corresponds to the account taken of the recombination of radical ion pairs and TTA, without including other interactions of active particles.

These aforementioned dependences were calculated in zero electric field. Signs « $\times$ » show the recombination rate of the geminate pairs  $D^{+\bullet}/e^-$  (Fig. 5a) and the rate of  $^3D^*$  collisions (Fig. 5b) in external electric field  $E = 24$  kV/cm. A dramatic decrease in  $D^{+\bullet}/e^-$  recombination rate caused by a comparatively low electric field is due to rather high electron mobility. On the other hand, a weak dependence of triplet–triplet collisions on the field strength is due to the fact that the major part of  $^3D^*$  appears via energy transfer from  $^1S^*$  to D and the subsequent intercombinational conversion of  $^1D^*$  via reactions (1)–(2)–(6)–(7). Since the escape of the ions into the bulk at  $E_0 = 24$  kV/cm is increased by several percent only and the major part of  $^1S^*$  arises from reaction (2) within a subnanosecond time domain, the number of  $^3D^*$  and their spatial distribution vary slightly with the turning the electric field on.

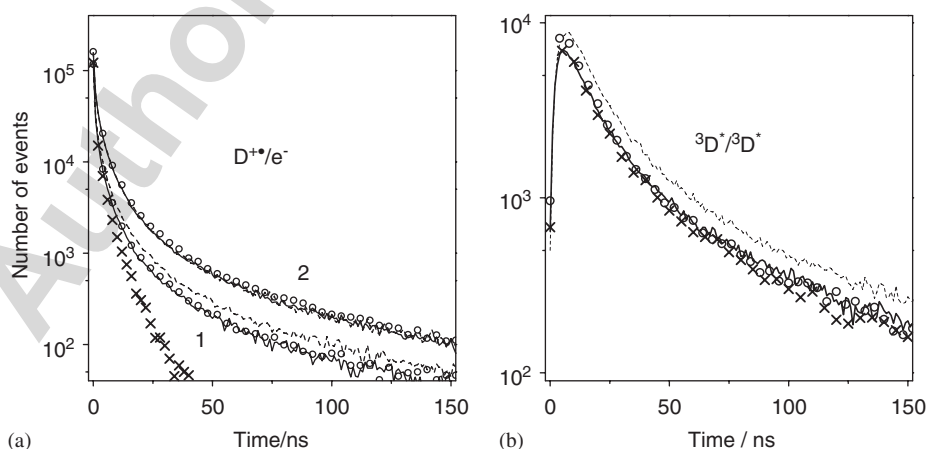


Fig. 5. (a) The recombination rate of geminate (curves 1) and cross (curves 2) pairs  $D^{+\bullet}/e^-$ . (b) The number of encounters between  $^3D^*$  per 1 ns. All the calculations are performed at  $N_0 = 5$ ,  $R_S = 5$  nm,  $[D] = 20$  mM for  $10^6$  cycles in zero electric field. The reactions, which were taken into account, were (1)–(25) (solid lines), only reactions (1)–(17) (circles), and only reactions (1)–(11) (dashed lines). The figure gives also the rate of geminate recombination of  $D^{+\bullet}/e^-$  pairs (5a, signs « $\times$ ») and the rate of triplet collisions (5b, signs « $\times$ ») at  $E_0 = 24$  kV/cm.

Comparison of the curves in Fig. 5a reveals that taking into account reactive species encounters leads to a decrease in the contribution of the recombination of geminate radical ion pairs in which the spin correlation can exist. In the framework of the used model, this is due to the convention that the spin exchange involving any partners of spin-correlated geminate radical ion pair with a particle having spin results in the spin coherence decay with a probability as given in Table 2.

An increase in the number of encounters between  $^3\text{D}^*$  (Fig. 5b) that appears after excluding reactions (12)–(25) from the consideration may be attributed to the fact that after the excluding the yield of  $^1\text{S}^*$  is increased and  $^1\text{D}^*$  yield via reaction (3) is also increased. As a result, the yield of the  $^3\text{D}^*$  becomes higher, too. It is worth noting that neglecting reactions (18)–(25) that describe the formation of neutral radicals has insignificant effect on the kinetics shown in Fig. 5. This is in agreement with the aforementioned conclusion that for the used model the collisions with electrons and solvent holes at the earliest stages of spur recombination have the major effect on the  $^1\text{S}^*$  yield.

Thus, although in the used model almost all excited solvent molecules are transformed into neutral radicals, what is the top estimate for alkanes, the encounters involving the primary charge carriers appear to dominate as regard to excited states formation.

### 3.4. Time-resolved effects of external fields

The external electric or magnetic fields were frequently applied to study the track structure and the primary radiation–chemical reactions. The electric field is known to increase the ion escape probability into the bulk and decrease the probability of their recombination (Freeman, 1987; Bartczak and Hummel, 1997; Anishchik et al., 1996). In turn, it results in the quenching of the delayed

fluorescence and allows one to separate the channels of the formation of excited states via the ion recombination.

The magnetic field effect is determined by spin-correlated geminate radical ion pairs. The magnetic field decreases the rate of the depopulation of the singlet state of the spin-correlated pairs thus leading to an increase in the yield of the singlet excited molecules and fluorescence intensity (Anisimov, 1991; Brocklehurst, 1997; Bagryansky et al., 2004). In zero magnetic field, the singlet-state population of  $\text{D}^+\cdot/\text{e}^-$  pair is assumed to be 0.25 due to the mixing among one singlet and three triplet spin states of the pair. In this work, by neglecting any spin-lattice relaxation process, we assume that in nonzero magnetic field, the mixing occurs only between the singlet state and the only triplet one. This doubles a relative population of the singlet state and the contribution of geminate pairs to fluorescence intensity in nonzero magnetic field.

In the time-resolved experiments, the influence of the external fields is typically analyzed using the relative change of fluorescence decay after the external field becomes nonzero. Fig. 6a shows such ratios  $I_F(t)/I_0(t)$ , where  $I_F(t)$  is the calculated intensity in the presence of electric (curves 1) or magnetic (curves 2) fields,  $I_0(t)$  is the intensity in the absence of the fields. These field effects were obtained for the same spur parameters as the curves shown in Fig. 5 were done ( $R_S = 5$  nm,  $N_0 = 5$ ,  $E = 24$  kV/cm) at  $[\text{D}] = 1$  and  $[\text{D}] = 20$  mM. Particular value of nonzero magnetic field is of no essence in the model used. A dashed line shows the calculated field effects with taking into account reactions (1)–(11), which is the first approximation to include pair collisions in a radiation spur.

As follows from Fig. 6a, for low acceptor concentrations, almost complete electric field quenching is reached, whereas at  $[\text{D}] = 20$  mM the time-resolved electric effect passes to plateau at about 0.3. The near-complete quenching of the contribution of  $\text{D}^+\cdot/\text{e}^-$  pairs recombination takes place

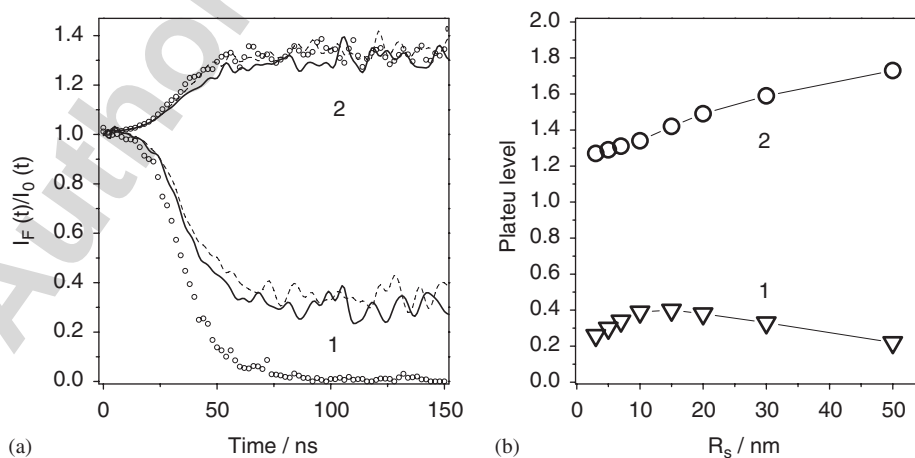


Fig. 6. (a) The ratios  $I_F(t)/I_0(t)$ , where  $I_F(t)$  is the calculated intensity in the presence of external, electric ( $E_0 = 24$  kV/cm, curves 1) or magnetic (curves 2) fields,  $I_0(t)$  is the intensity in the absence of external fields. The figure shows the field effects at  $[\text{D}] = 1$  mM (circles) as well as at  $[\text{D}] = 20$  mM (lines) when taken into account are all of reactions (1)–(25) (solid line) or only reactions (1)–(11) (dashed line).  $R_S = 5$  nm,  $N_0 = 5$ . (b) The dependence of the mean plateau level over the range 100–150 ns for electric (curve 1) and magnetic (curve 2) effects at  $[\text{D}] = 20$  mM on  $R_S$  value.  $N_0 = 5$ .

also at higher acceptor concentration, and the plateau level actually shows the contribution of TTA in the delayed fluorescence at times longer than 50 ns. As for magnetic field effect, as it was mentioned above, the exceeding of magnetic effect level over unity is approximately equal to the relative contribution of the geminate recombination of  $D^{+\bullet}/e^-$  pair to fluorescence intensity.

It is worth noting that both the electric and magnetic fields affect the fluorescence intensity with a delay in the early times. This delay takes place because the significant portion of the intensity at this time range appears via energy transfer (6), which depends weakly on the external fields. As for the weak influence of the active particles encounters on the field effects, this may be explained by a synchronism in the influence of reactions (12)–(25) on both spin-correlated geminate ion recombination and TTA. As it was demonstrated above with Figs. 5a and b, taking into consideration reactions (12)–(25) one reduces both of the channels, thus leading to minor effect of the encounters on the magnitudes of the time-resolved electric field effects and to almost complete compensation of that in the case of magnetic field effects. Note that the encounters involving neutral radical contribute to the change of  $^1D^*$  fluorescence kinetics negligibly as compared to other intermediates.

Fig. 6b presents the results of calculations of the plateau levels of electric (curve 1) and magnetic (curve 2) field effects for a solution containing 20 mM of acceptor, for  $N_0 = 5$  but for different radii of the spur. The plateau levels were determined as a mean value of the effects over the range 100–150 ns.

The magnetic field effect increases with decreasing local ionization density and tends to 2. This is in agreement with known results (Anisimov, 1991; Brocklehurst, 1997) and is assigned to an increase in the geminate recombination probability in a spur. In a very compact spur, due to TTA contribution the maximum of magnetic effect in excess of unity is smaller than  $1/N_0$ .

For the case of the plateaus of electric field effects one can see that these vary nonmonotonically with increasing spur size. Such a behavior can be assigned to the nonmonotonically changing contribution of TTA, which is due to interplay of several factors. Among them are these:

- (1) When going to smaller spurs and higher density of the local ionization, the effective decay of  $^1S^*$  at short times leads to significant decrease in the yield of  $^1D^*$  and, subsequently,  $^3D^*$ ;
- (2) The reaction of TTA is nonhomogeneous one and its rate at larger initial distance between triplets, for sufficiently long time, becomes slightly higher as compared to the case of smaller initial distance;
- (3) In the spur of very large radius, the probability of triplet molecules encounter is very small within the time domain under study and TTA process does not contribute significantly to the intensity.

#### 4. Conclusions

Computer simulation of the formation of the singlet excited solutes in alkane solution of an electron donor, which is also an electronic excitation energy acceptor and luminophor, shows that:

- (1) In the spurs under consideration, contact interactions that accelerate the conversion of singlet excited solvent molecules to triplet ones at early times are mostly the encounters of the excited molecules with primary charge carriers. These are the main factor, which determines the yield of the singlet excitations. Encounters with neutral radicals become more important in later moments and these result in a moderate shortening of the “observed” fluorescence lifetime of the singlet excited states.
- (2) The contribution of the annihilation of triplet solutes formed in the same spur to the delayed fluorescence intensity becomes comparable with that of the radical ion pairs recombination within nanosecond time range at the luminophor concentration of about 10 mM and this increases with the concentration.
- (3) The formation of neutral radicals in a spur via the decay of triplet excited solvent molecules does not affect significantly the curves of the time-resolved electric or magnetic field effects.

#### Acknowledgments

The authors are grateful to Prof. Yu.N. Molin, Dr. V.A. Bagryansky and Dr. F.B. Sviridenko for fruitful remarks and suggestions that allowed us to improve the present work. This work was supported by the Russian Foundation for Basic Research (Grant 04-03-32161), and the program of ‘Leading Science Schools’ (Grant NS-5078.2006.3).

#### References

- Anishchik, S.V., Borovkov, V.I., Anisimov, O.A., 1996. On the feasibility of identifying the formation mechanism of secondary cations by means of electric field quenching recombination fluorescence. *High Energy Chem.* 30, 397.
- Anisimov, O.A., 1991. Ion pairs in liquids. In: Lund, A., Shiotani, M. (Eds.), *Radical Ionic Systems*. Kluwer Academic Publishers, Dordrecht, The Netherlands, pp. 285–309.
- Bagryansky, V.A., Borovkov, V.I., Molin, Yu.N., 2004. Spectroscopic capabilities of the time-resolved magnetic field effect technique as illustrated in the study of hexamethylethane radical cation in liquid hexane. *Phys. Chem. Chem. Phys.* 6, 924–928.
- Barigelletti, F., Dellonte, S., Mancini, G., Orlandi, G., 1979. On the energy-transfer rate parameters of liquid alkanes. *Chem. Phys. Lett.* 65, 176–180.
- Bartczak, W.M., Hummel, A., 1993. Formation of singlet and triplet excited states on charge recombination in tracks of high-energy electrons in nonpolar liquids; a computer simulation study. *Chem. Phys. Lett.* 208, 232–236.

- Bartczak, W.M., Hummel, A., 1997. Computer simulation of charge recombination in model tracks of high-energy electrons in nonpolar liquids; kinetics and escape. *Radiat. Phys. Chem.* 49 (6), 675–687.
- Borovkov, V.I., Anishchik, S.V., Anisimov, O.A., 1997. Time-resolved electric field effects in recombination fluorescence as a method of studying primary radiation–chemical processes. *Chem. Phys. Lett.* 270, 327–332.
- Borovkov, V.I., Anishchik, S.V., Anisimov, O.A., 2003. Mobility of geminate radical ions in concentrated alkane solutions as measured using electric field dependence of delayed fluorescence. *Rad. Phys. Chem.* 67, 639–650.
- Brocklehurst, B., 1992a. Model calculation on hydrocarbon radiolysis. Part 1. Spin correlation effects in pure alkanes. *J. Chem. Soc. Faraday Trans.* 88 (2), 2823–2832.
- Brocklehurst, B., 1992b. Model calculation on hydrocarbon radiolysis. Part 2. Excited states in solutions of aromatics in alkanes. *J. Chem. Soc. Faraday Trans.* 88 (9), 2823–2832.
- Brocklehurst, B., 1997. Spin correlated and magnetic field effects in radiolysis. *Radiat. Phys. Chem.* 50, 213–225.
- Freeman, G.R., 1987. Ionization and charge separation in irradiated materials. In: Freeman, G.R. (Ed.), *Kinetics of Nonhomogeneous Processes*. Wiley, New York, pp. 19–87.
- Gee, N., Senanayake, P.C., Freeman, G.R., 1988. Electron mobility, free ion yields, and electron thermalization distances in alkane *n*-liquids: effect of chain length. *J. Chem. Phys.* 89, 3710–3717.
- Holroyd, R.A., Sham, T.K., 1985. Ion yields in hydrocarbon liquids exposed to X-rays of 5–30-keV energy. *J. Phys. Chem.* 89, 2909–2913.
- Holroyd, R.A., Preses, J.M., Hanson, J.C., 1997. Excited singlet-state yields in hydrocarbon liquids exposed to X-rays. *J. Phys. Chem. A* 101, 6931–6935.
- Hong, K.M., Noolandi, J., 1978. Solution of the time-dependent Onsager problem. *J. Chem. Phys.* 69, 5026–5039.
- Hummel, A., Bartczak, W.M., 1988. The contribution of multiple ion pairs to ion recombination in irradiated nonpolar liquids; a computer simulation study. *Radiat. Phys. Chem.* 32, 137–142.
- LaVerne, J.A., Pimblott, S.M., Wojnarovits, L., 1997. Diffusion-kinetic modeling of  $\gamma$ -radiolysis of liquid cycloalkanes. *J. Phys. Chem. A* 101 (8), 1628–1634.
- Lozovoy, V.V., Anishchik, S.V., Medvedev, N.N., Anisimov, O.A., Molin, Yu.N., 1990. Monte Carlo modelling of radical ion recombination in multiparticle tracks. *Chem. Phys. Lett.* 167, 122–128.
- Mehnert, R., 1991. Radical cations in pulse radiolysis. In: Lund, A., Shiotani, M. (Eds.), *Radical Ionic Systems*. Kluwer Academic Publishers, Dordrecht, The Netherlands, pp. 231–284.
- Mehnert, R., Brede, O., Naumann, W., Hermann, R., 1988. The mechanism of singlet energy transfer from alkanes. *Radiat. Phys. Chem.* 32 (3), 325–328.
- Molin, Yu.N. (Ed.), 1984. *Spin Polarization and Magnetic Field Effects in Radical Reactions*. Elsevier, Amsterdam.
- Mozumder, A., 1999. *Fundamentals of Radiation Chemistry*. Academic Press, San Diego, London.
- Okamoto, M., Teratsuji, T., Tazuke, Y., Hirayama, S., 2001. Effect of pressure on intersystem crossing between the encounter complex pairs involved in triplet–triplet annihilation of 2-acetonaphthone in liquid solution. *J. Phys. Chem. A* 105 (18), 4574–4578.
- Ovchinnikov, A.A., Timashev, S.F., Belyy, A.A., 1989. *Kinetics of Diffusion Controlled Chemical Processes*. Nova Science, Commack, NY, 215pp.
- Pimblott, S.M., Green, N.J.B., 1996. Simulation of ion recombination in low permittivity solvents: extended clusters. *Radiat. Phys. Chem.* 47, 233–240.
- Potashnik, R., Ottolenghi, M., Bensasson, R., 1969. Photoionization and delayed fluorescence in liquid solutions of *N,N,N',N'*-tetramethyl-*p*-phenylenediamine. *J. Phys. Chem.* 73 (6), 1912–1918.
- Rothman, W., Hirayama, F., Lipsky, S., 1973. Fluorescence of saturated hydrocarbons. III. Effect of molecular structure. *J. Chem. Phys.* 58 (4), 1300–1317.
- Sauer Jr., M.C., Jonah, C.D., 1994. The ratio of triplet to singlet excited state formation from ion recombination in the radiolysis of aromatic solutes in alkane liquids. *Radiat. Phys. Chem.* 44, 281–295.
- Sauer Jr., M.C., Jonah, C.D., Naleway, C.A., 1991. Study of the reactions of geminate ions in irradiated scintillator, hydrocarbon solutions using recombination fluorescence and stochastic simulations. *J. Phys. Chem.* 95, 730–740.
- Schmidt, K.H., 1983. DC conductivity and geminate ion recombination in irradiated hydrocarbons: model calculation. *Chem. Phys. Lett.* 103, 129–132.
- Schwarz, F.P., Smith, D., Lias, S.G., Ausloos, P., 1981. The fluorescence and photofragmentation of liquid saturated hydrocarbons at energies above the photoionization threshold. *J. Chem. Phys.* 75 (8), 3800–3808.
- Shkrob, I.A., Sauer Jr., M.C., Trifunac, A., 2001. Radiation chemistry of organic liquids: saturated hydrocarbons. In: Jonah, C.D., Rao, B.S.M. (Eds.), *Radiation Chemistry: Present Status and Future Trends*. Elsevier, Amsterdam, pp. 175–221.
- Siebbeles, L.D.A., Bartczak, W.M., Terrissol, M., Hummel, A., 1997. Computer simulation of the ion escape from high-energy electron tracks in nonpolar liquids. *J. Phys. Chem. A* 101, 1619–1627.
- Singh, A., 1972. Triplet state formation in pulse radiolysis. *Radiat. Res. Rev.* 4, 1–69.
- Terazima, M., Okazaki, T., Hirota, N., 1995. Translational diffusion process of charged radicals: *N,N,N',N'*-tetramethyl-*p*-phenylenediamine and its cation radical. *J. Photochem. Photobiol. A: Chem.* 92, 7–12.
- Ukai, A., Hirota, N., Terazima, M., 2000. Diffusion of organic molecules in the excited triplet states detected by the transient grating with a high wavenumber. *J. Phys. Chem. A* 104 (29), 6681–6688.
- Yoshida, Y., Tagawa, S., Tabata, Y., 1991. Geminate ion recombination in nonpolar liquid. In: Tabata, Y. (Ed.), *Pulse Radiolysis*. CRC press, Boca Raton, FL, pp. 343–355.